Acoustic Emission During Austenite $\rightarrow \varepsilon$ Martensitic Phase Transformation in TWIP/TRIP Steels



M.K. BOLGÁR, E. NAGY, L. DARÓCZI, M. BENKE, V. MERTINGER, and D.L. BEKE

Acoustic emission in two different TWIP/TRIP steels during thermally induced γ – ε martensitic phase transformation was investigated. Large asymmetry was observed: the noise activity was considerably larger for heating than cooling. This was explained by the plastic deformation and strain-induced martensite nucleation (which usually provides much lower acoustic emission signals) in the austenite during cooling. The amplitude and energy probability distribution functions for heating followed the power-law behavior, and the critical exponents were counted as well. The amplitude and energy exponents (α and ε , respectively) for the two different samples were the same within the errors ($\alpha = 2.4 \pm 0.2$, $\varepsilon = 1.7 \pm 0.1$), indicating the universal character. The acoustic activity νs martensite volume faction showed a maximum at around 60 pct for heating, which is most probably related to the coming apart of the elastic fields of the martensite variants.

https://doi.org/10.1007/s11661-019-05291-0 © The Author(s) 2019

I. INTRODUCTION

TWINNING-INDUCED plasticity (TWIP) and transformation-induced plasticity (TRIP) steels are important because they exhibit high deformability and strength at the same time. In such steels the austenite is able to accommodate strain through both dislocation glide and twinning on the $\{111\}_{\nu}\langle 112\rangle_{\nu}$ slip system. In these alloys (typically containing large amounts of Mn (15 to 30 wt pct)^[1-3]) the perfect a/2 (011) γ dislocations dissociate into Shockley partials on the close packed $\{11\overline{1}\}_{v}$ plane with a stacking fault forming between the partials.^[1] The faulted region is a plate of the strain-induced ε-martensite with a hexagonal close-packed crystal structure. TWIP steels exhibit rather low yield strength, but their ultimate tensile strength can exceed 1100 MPa. This is due to their high strain-hardening coefficient, which results in large uniform elongation (60 to 95 pct).[1-6] The high degree of strain-hardening is considered to be the result of the competition between the dislocation slip and ε -martensite formation. [2–6] In

processes being undergone is necessary. Thus, investigations of the details of the martensitic transformations are desired. In this work the austenite-martensite transformation was monitored with acoustic emission (AE), which can furnish significant data about the elementary jumps of the intermittent martensitic transformations. The AE events are transient elastic waves due to a sudden release of the energy from localized sources within a material, and they can be detected by acoustic sensors placed on the surface of the specimen. Although acoustic emission measurements are used in the literature to investigate the thermal- or strain-induced martensitic transformations in different steels,[9-11] in most cases the root mean square (RMS) values of AE jerks or the AE energy emitted during the transformation were analyzed and correlated with the martensite

volume fraction. In recent publications on AE, [8,12,13]

the analysis goes beyond extracting only the above

average information. It contains both the statistical

analysis of AE jerks (by plotting the probability distributions of the elementary AE peaks^[12]) and the

analysis of the shapes of the individual AE events (which

can lead to identification of different clusters of signals

TRIP steels the misfit, accompanied by the stress or thermally induced formation of martensite nuclei, leads

to the plastification of the neighboring austenite regions^[7] by formation of ε -martensite as the result of

extended and overlapping stacking faults. [8] As a result,

TRIP steels are characterized by concurrently high

strength and high ductility. The above-mentioned excep-

tional properties of TWIP and TRIP steels are beneficial

for many different applications (see, e.g., Reference 2). To exploit this potential, a better apprehension of the

Manuscript submitted February 15, 2019. Article published online May 29, 2019

M.K. BOLGÁR, L. DARÓCZI, and D.L. BEKE are with the Department of Solid State Physics, University of Debrecen, P.O. Box 400, Debrecen 4002, Hungary. Contact e-mail: dbeke@science.unideb.hu E. NAGY is with the MTA-ME Materials Research Group, University of Miskolc, Miskolc-Egyetemváros 3515, Hungary. M. BENKE and V. MERTINGER are with the Institute of Physical Metallurgy Metalforming and Nanotechnology, University of Miskolc, Miskolc-Egyetemváros, 3515, Hungary.

of the same origin^[8,13]). Thus, such measurements can provide further information on the details of the dynamics of the martensitic transformations. For example, it yields data on the dependence of the AE activity on the transformed martensite volume fraction (see, e.g., Reference 14) or on the asymmetry of the transformation, which is manifested in the difference of the number of AE events during the forward (i.e., from austenite to martensite) as well as reverse transformations.^[15] In addition, the above asymmetry is also clearly manifested in differences of the critical exponents of the energy or amplitude distribution functions. AE shows a self-similar behavior leading to power law distributions with characteristic exponents, [16,17] since the jerky character of the martensitic transformations (MTs) is related to the intermittent formation of martensite variants during cooling (or their disappearance during heating). This is characterized by avalanches, which can be described by power law distributions^[16,17]

$$P(x) \sim x^{-\beta} \exp\left(-\frac{x}{x_c}\right),$$
 [1]

where P(x) is the probability density of the x parameter (number of events with a given x value divided by the number of all events). x can be the amplitude, size, energy or duration of the jerks, β is the corresponding critical exponent, and x_c is the cutoff value.

While carrying out such a sophisticated statistical analysis of AE noises emitted during martensitic transformations in shape memory alloys^[14,18,19] has become increasingly popular and there are many publications on the strain-induced martensitic transformations (see, e.g., References 8, 9, and 20 through 22), to the authors' knowledge there is only one communication in which the critical exponent of the energy distribution was calculated during strain-induced martensitic transforaustenitic in 304L stainless $(\varepsilon = 1.75 \pm 0.15)$. Thus, our aim was also to carry out the above statistical analysis of the obtained AE noises, for the first time, during thermally induced transformation.

II. EXPERIMENTAL

TWIP/TRIP steel samples with two different Cr contents were investigated. The compositions are shown in Table I. The samples were provided by the University of Freiberg as hot-rolled rods with a 12-mm diameter. Discs were cut from the rods and were subsequently heat treated (austenized) at 1273 K for 30 minutes in nitrogen and then water quenched. According to previous

Table I. Composition of the Investigated Steels (Weight Percent)

Steel	С	Mn	Cr	Si	S	P
A	0.02	17.7	2.26	0.1	0.029	0.0051
B	0.08	17.7	6.12	0.06	0.025	0.003

examinations, the as-quenched samples mainly consisted of ε-martensite (80 pct) and some austenite. [23] Preliminary experiments had indicated that the grain size had a potent influence on the AE detected (it was higher at larger grain sizes). To increase the grain size, heat treatments were made at 1000 °C for 24 hours. After the heat treatments 15 cycles of the γ - ε martensitic phase transformation were made to reach the stationary state of the transformation. [24] No deformation was applied to the samples, so only thermally induced processes contributed to the transformation. The mass of the samples investigated was 226 mg (steel A) and 197 mg (steel B), respectively. The acoustic emission measurements were carried out in a modified DSC device (10 K/ min driving rate) with Sensophone AED 404 Acoustic Emission Diagnostic Equipment (Geréb Co., Ltd., Hungary) with piezoelectric sensors. The threshold level was determined from a measurement carried out in a martensitic state without heating/cooling (i.e., when the low-level acoustic emission should not belong to the phase transformation) and was set to 37 dB. The A/D converter sampling rate was 16 MHz, and the setup had a band pass from 30 kHz to 1 MHz. A 30 dB preamplifier and a maximum 100 dB main amplifier were used. For the computation of the exponents logarithmic data binning (the whole interval was split into 40 bins) was used. The DSC curves of the austenite-martensite transformation and the hysteresis curves for steels A and B are shown in Figure 1. The heats of transformation for cooling and heating are $Q_{\rm cA}=-11600~{\rm J/kg},$ $Q_{\rm cB}=-8700~{\rm J/kg},$ $Q_{\rm hA}=12~600~{\rm J/kg}$ and $Q_{\rm hB}=8~600~{\rm J/kg},$ respectively. The magnitude of the transformation entropies was determined in a similar way as the hysteresis curves (see, e.g., Reference 25) and was taken as the arithmetic mean of the magnitudes of values obtained from the forward and reverse transformation. This yielded 28 and 21 J/kg K for steel A and B, respectively (ΔS is negative for the austenite to martensite transformation).

The optical images were taken with a Zeiss Axio Scope A1 microscope in differential interference contrast mode. The samples were etched in a 3 pct nital solution for 10 seconds before the microscopic investigation.

III. RESULTS AND DISCUSSION

The change of the grain size in steel B after the 24 hour heat treatment is shown in Figure 2. It can be seen that during the high-temperature treatment the average grain size increased drastically (from about 1 to $100~\mu m$). This treatment was necessary to detect sufficient acoustic emission from the samples during the phase transformation. In the original state the emitted signals were close to or below the threshold level, but after the heat treatment the acoustic activity considerably increased above the threshold level and became well detectable.

Figure 1 shows that the hysteresis curve is very wide (corresponding to a large dissipative energy of transformation), while the slopes of the cooling and heating branches only slightly deviate from that of a vertical

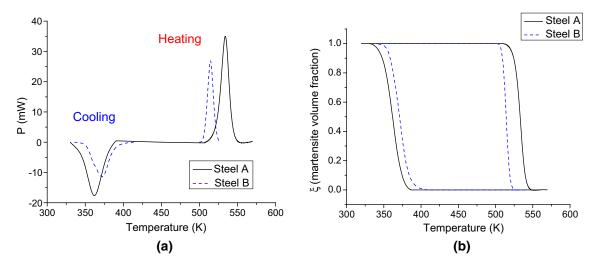


Fig. 1—(a) DSC curves of the austenite-martensite and reverse transformation and (b) the hysteresis curve in steel A and B (heating/cooling rate 10 K/min).

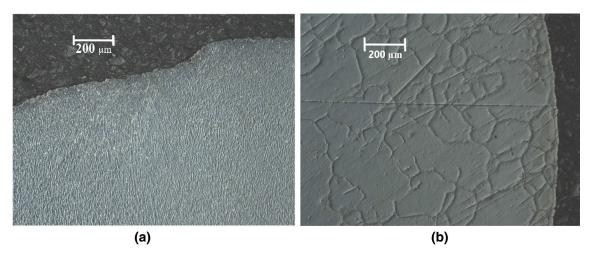


Fig. 2—Grain structure of steel B (a) before and (b) after the 1000 °C 24-h heat treatment, differential interference contrast.

line, which would belong to a small elastic energy contribution to the heats of transformation.^[25] In addition, the shapes of the DSC peaks are similar to those obtained in Reference 24: the peaks for heating are sharper than for cooling.

The measured acoustic noise during heating and cooling in steel A is shown in Figure 3, which shows that while during heating the acoustic activity is relatively high and well-correlated with the γ – ε transformation, during cooling only a few small noise packages were detected. This asymmetric behavior had not been detected before in steels and is contrary to our acoustic noise measurements in shape memory alloys, where usually the activity during cooling was more eminent. ^[15,26]

The probability distribution functions were calculated from the data obtained during heating after measuring some (\sim 10) cycles in both A and B steels. Figure 4 shows a typical AE wave packet, with the usual definitions of the evaluated parameters. The energy of an individual acoustic event, E_i , was determined from an

approximate integration taking half of the product of the square of the voltage signal with the duration time. The total acoustic energy is the sum of energies of the individual acoustic events above the threshold level. The calculated amplitude and energy distribution functions during heating for the two samples are shown in Figure 5. Note that the distribution functions follow the power law in five orders of magnitude range, indicating that the power law provides a good fit even by neglecting the cutoff. The critical amplitude and energy exponents are the same (within error) for the two types of steels ($\alpha = 2.4 \pm 0.2$, $\varepsilon = 1.7 \pm 0.1$; the errors correspond to the limit within which the slopes of two subsequent measurements were the same). In addition, the critical exponents fulfill the well-known scaling rule^[16]: $(\alpha - 1)/(\epsilon - 1) = 2$.

Table II shows the number of events for both samples. Since these parameters are not comparable because of the different AE sensor-sample connections, the ratios of the heating and cooling values were calculated. It can be seen that the ratios of the number

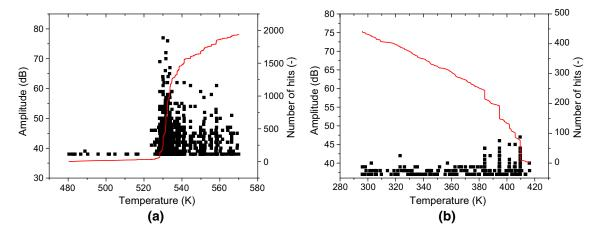


Fig. 3—(a) Activity of acoustic noise measured during heating and (b) cooling in steel A. Points indicate the amplitudes of individual hits, while the continuous curve gives the sum of events.

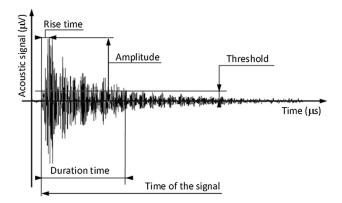


Fig. 4—Typical wave packet of an acoustic signal and the measured parameters, reprinted from Ref. [14].

of events and total energies for heating and cooling are considerably larger than unity (negative asymmetry, i.e., the number of events is smaller for cooling than heating. and the values of μ and ξ are larger than unity^[15]). This is in agreement with the acoustic activity shown in Figure 3 and also indicates that even the determination of the critical exponents is difficult for cooling: very small numbers of hits were detected, and the amplitudes were also too small. Nevertheless, the energy probability distribution function for cooling in steel B is shown in Figure 6. It is worth noting that the energy scale is much narrower (covers only about two orders of magnitude) than for heating. Nonetheless, the points approximately follow a straight line, although the points at smaller energy values have quite large uncertainty and are influenced by the choice of the threshold. The red line in Figure 6 illustrates the linear fit: the slope is $\varepsilon = 1.9$, but the error bars of ε are large enough (\pm 0.3). The very large negative asymmetry suggested by the γ and μ values (much larger than unity) is remarkable and is due to the very low activity detected for cooling.

For the interpretation of the above large asymmetry, we have to take into account the results of References 23 and 27. Optical microscopic investigations (on an alloy having 21.03Mn, 6.53Cr, 0.08C, 0.07Si, 0.03P, 0.03S

composition close to our B, except the higher Mn content and the different cooling rate, 40 K/min^[23]) revealed that the changes of the surface relief, accompanied by the martensitic transformation, showed a characteristic development with the number of cooling/ heating cycles. Since our measurements were carried out after the first 15 cycles, we have to consider the results obtained during the 14th cycle (see Figure 3 in Reference 23). First, it was observed that the ε phase always formed at the same location, where it disappeared during heating, i.e., preferred nucleation centers were formed/activated. Second, during the $\gamma \to \varepsilon$ transformations plastic deformations in the austenite were observed. Third, the relief change during cycling became less and less notable, i.e., plastic deformation occurred in every cycle. In addition, Reference 27 shows that the heating DSC curves were considerably wider for samples containing both thermally and strain-induced ε martensite than for those belonging to the dissolution of the only thermally induced martensite.

It is worth noting that the asymmetry in shape memory alloys was interpreted in Reference 15 by the different ways of relaxation of the elastic strain energy during cooling as well as heating. It was assumed that the dissipative energy contributions are the same in both directions and are small compared to the relaxed fractions of the elastic energies stored during the phase transformation (as it is usually assumed in thermoelastic transformations taking place in shape memory alloys). In general, this is not the case for martensitic transformations in steels where plastic deformation can be accompanied by the phase transition. Optical microscopic observations of samples, with similar compositions to our B sample, [23] indicated that this is indeed the case, suggesting that the phase transformation-induced plasticity is responsible for the large asymmetry.

Figure 7 shows the acoustic activity as a function of the martensite volume fraction. The martensite volume fractions were calculated from the corresponding fractions of the transformation entropy calculated from the DSC measurements. [25] The error bars are the same for cooling and heating; however, because of the small

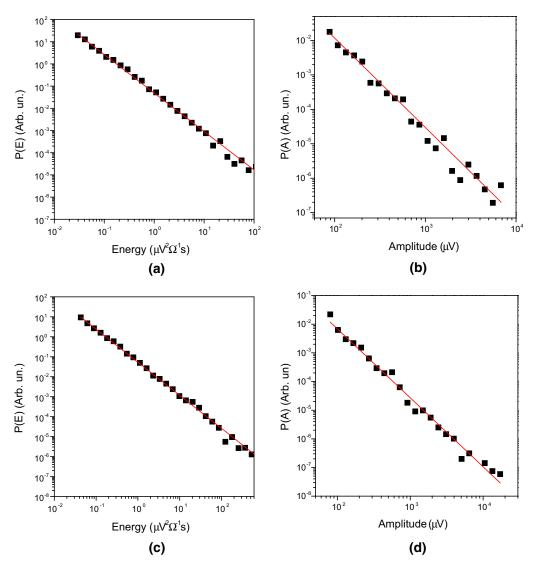


Fig. 5—The probability distribution functions during heating. (a and b) Energy and amplitude distributions for steel A, respectively. (c and d) Energy and amplitude distributions for steel B, respectively.

Table II. The Number of Events for One Cycle (Heating and Cooling) in Steel A and B

	Number	of events		
	Heating $N_{\rm h}$	Cooling N _c	$\mu=rac{N_{ m h}}{N_{ m c}}$	$\gamma = \frac{E_{\rm h}}{E_{\rm c}}$
Steel A Steel B	1935 1854	441 468	4.39 3.96	202 142

The γ and μ are asymmetry parameters describing the ratio of the total acoustic energies and events during heating and cooling.

absolute values, the activity-scale is much more stretched for cooling. The plot for cooling is almost flat (with a small peak at about 90 pct martensite volume fraction), if we take into account the error bars, too. At the same time, it can be seen that there is a maximum at about 60 pct martensite volume fraction for heating.

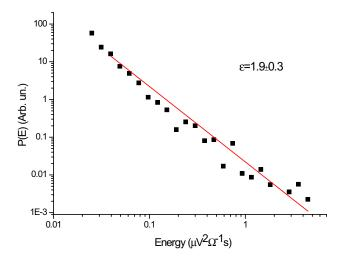


Fig. 6—The energy probability distribution function during cooling in steel B.

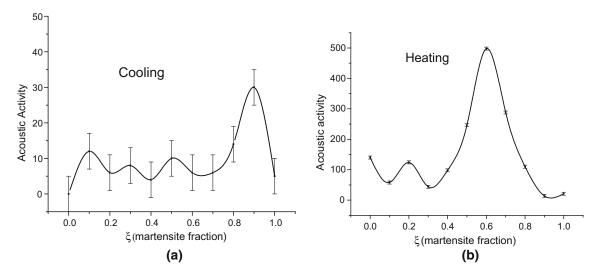


Fig. 7—Acoustic activity vs the martensite volume fraction in steel B (a) for cooling and (b) heating. The continuous lines are just to guide the eye. The error bars were determined from the average differences between two subsequent measurements.

For the interpretation we offer the following possible explanation. During cooling, if the stress field—developed by the formation of the primary martensite needles—is larger than the critical stress, plastic deformations start in the austenite which leads to strain-induced ε formation ($\varepsilon_{\rm str}$ phase), too. This serves as easy nucleation centers for the thermally induced ε during further cooling (our DSC peaks for heating are sharp, indicating the presence of one thermally induced ε phase). Thus, the elastic energy stored during cooling should be small, and the dissipated part should be large in accordance with Figure 1(a). At the same time, there is a chance for direct nucleation/growth of thermally induced martensite needles, which produces rare "normal" AE signals from the usual intermittent motion of the interface between the ε and γ phases. On the other hand, during heating there is no plastic deformation of the freshly formed austenite (the small stresses, stored during cooling, gradually relax), and the phase transformation is realized by nucleation/intermittent motion of interfaces free from plastic deformation.

The interpretation of the asymmetry observed in the acoustic emission is based on the above picture. The low AE activity during cooling can be the consequence of the much lower acoustic emission during plastic deformation-induced nucleation of the ε_{str} martensite (see, e.g., Reference 13) compared with the thermally induced nucleation and growth. During heating there is practically no plastic flow, and the transformation takes place by nucleation/intermittent motion of the interfaces. Thus, it is also not surprising that the energy exponents are similar for heating and cooling, since both can be related to thermally induced nucleation of ε and/or intermittent motion of the austenite/martensite interface. Since during cooling the volume fraction of such directly nucleated martensite, compared with the volume fraction of the ε phase formed from the deformation-induced ε_{str} martensite, is small, the overall AE activity is low for cooling. The peak during heating at about 60 pct martensite volume fraction can also be accompanied by the relaxation of the elastic energy stored during the formation of the thermally induced ε phase.

It is interesting that the energy exponent determined from only one AE measurement during strain-induced martensite formation in 304L austenitic stainless steel $(\varepsilon = 1.75 \pm 0.15)^{[12]}$ is in good accordance with our values. Since the AE signals in both experiments originated from the $\rightarrow \varepsilon$ transformation, this agreement is in accordance with the universal character of power law behavior. This suggests that the values of the critical exponents are the same for transformations with the same symmetry change and depend only slightly on the type of phase transformation (on the symmetry change). The same arguments can be applied to the similar values obtained in the A and B samples.

IV. CONCLUSIONS

- The intermittent character of the martensitic transformation during heating leads to clear power law behavior of the probability density distributions of the amplitudes and energies of acoustic emission events.
- 2. Surprising asymmetry is observed: the AE activity was considerably larger for heating than cooling. In the latter case it was only slightly above the background noise, and thus the critical exponents could be more reliably calculated for heating. Most probably the large asymmetry is the consequence of the plastic deformation of the austenite during cooling, leading to deformation-induced nucleation of the ε phase. Thus, during cooling only a small fraction of the martensite grows by a thermally induced nucleation and growth process, and the AE activity is low, since the plastic deformation usually leads to very-low-amplitude AE signals.

- 3. The critical exponents were the same for the two alloys investigated and agree well with the energy exponent determined from AE measurements during strain-induced martensite formation in 304L austenitic stainless steel. This is in accordance with the universal character of the power law behavior, since both results belong to the γ-ε transformation.
- 4. The acoustic activity vs the martensite volume faction showed a maximum at around 60 pct for heating, which can be related to the relaxation of the elastic energy stored during cooling. Understanding of this calls for more detailed investigation of the correlation with the microstructural changes taking place during the martensitic transformation.

ACKNOWLEDGMENTS

Open access funding provided by University of Debrecen (DE). The work was supported by the GINOP-2.3.2-15-2016-00041 project. The project was co-financed by the European Union and the European Regional Development Fund. The described research was also supported through the National Research, Development and Innovation Office NKFIH K119566 and NKFIH 131541 project. Supported by the ÚNKP-17-3 New National Excellence Program of the Ministry of Human Capacities.

OPEN ACCESS

This article is distributed under the terms of the Creative Commons Attribution 4.0 International License (http://creativecommons.org/licenses/by/4.0/), which permits unrestricted use, distribution, and reproduction in any medium, provided you give appropriate credit to the original author(s) and the source, provide a link to the Creative Commons license, and indicate if changes were made.

REFERENCES

 H.K.D.H. Bhadeshia and R.W.K. Honeycombe: Steels Microstructure and Properties, 3rd ed., Butterworth-Heinemann, Oxford, 2006, p. 229.

- 2. B.C. De Cooman, Y. Estrin, and S.K. Kim: *Acta Mater.*, 2018, vol. 142, pp. 283–362.
- 3. L. Chen, Y. Zhao, and X. Qin: *Acta Metall. Sin.*, 2013, vol. 26, pp. 1–15.
- 4. P. Zhou and M.X. Huang: *Metall. Mater. Trans. A*, 2015, vol. 46A, pp. 5080–90.
- 5. T.T. Huang, W.J. Dan, and W.G. Zhang: *Metall. Mater. Trans. A*, 2017, vol. 48A, pp. 4553–64.
- P. Lan and J. Zhang: Metall. Mater. Trans. A, 2018, vol. 49A, pp. 147–61.
- 7. F.D. Fischer, Q.-P. Sun, and K. Tanaka: *Appl. Mech. Rev.*, 1996, vol. 49, pp. 317–64.
- 8. M. Linderov, C. Segel, A. Wiedner, H. Biermann, and A. Vinogradov: *Mater. Sci. Eng. A*, 2014, vol. 597, pp. 183–93.
- 9. S.M.C. van Bohemen, J. Sietsma, M.J.M. Hermans, and I.M. Richardson: *Acta Mater.*, 2003, vol. 51, pp. 4183–96.
- 10. S.M.C. van Bohemen, M.J.M. Hermans, and G. den Ouden: *Mater. Sci. Technol.*, 2002, vol. 18, pp. 1524–28.
- 11. S.M.C. van Bohemen, M.J.M. Hermans, G. den Ouden, and I.M. Richardson: *J. Phys. D*, 2002, vol. 35, pp. 1889–94.
- M. Shaira, N. Godin, P. Guy, L. Vanel, and J. Courbon: *Mater. Sci. Eng. A*, 2008, vol. 492, pp. 392–99.
- 13. A. Vinogradov, A.V. Danyuk, D.L. Merson, and I.S. Yasnikov: *Scr. Mater.*, 2018, vol. 151, pp. 53–56.
- L.Z. Tóth, L. Daróczi, S. Szabó, and D.L. Beke: *Phys. Rev. B*, 2016, vol. 93, pp. 144108–17.
- D.L. Beke, M.K. Bolgár, L.Z. Tóth, and L. Daróczi: *J. Alloys Compd.*, 2018, vol. 741, pp. 106–15.
- M.L. Rosinberg and E. Vives: Disorder and Strain-Induced Complexity in Functional Materials, Springer, Berlin, 2012, pp. 249–72.
- 17. A. Dobrinevski, P.L. Doussal, and K.J. Wiese: *EPL (Europhys. Lett.)*, 2014, vol. 108, pp. 66002–08.
- A. Planes, L. Mañosa, and E. Vives: J. Alloys Compd., 2013, vol. 577, pp. S699–S704.
- M.K. Bolgár, L. Daróczi, L.Z. Tóth, E.E. Timofeeva, E.Y. Panchenko, Y.I. Chumlyakov, and D.L. Beke: *J. Alloys Compd.*, 2017, vol. 705, pp. 840–48.
- L. Krüger, S. Wolf, U. Martin, S. Martin, P.R. Scheller, A. Jahn, and A. Weiss: *J. Phys. Conf. Ser.*, 2010, vol. 240, pp. 012098–012102.
- 21. A. Jahn, A. Kovalev, A. Weiss, S. Wolf, L. Krüger, and P.R. Scheller: *Steels Res. Int.*, 2011, vol. 82, pp. 39–44.
- J. Talonen and H. Hänninen: Acta Mater., 2007, vol. 55, pp. 6108–18.
- M. Benke, V. Mertinger, and F. Tranta: *Mater. Sci. Forum*, 2013, vols. 738–739, pp. 257–61.
- V. Mertinger, M. Benke, E. Nagy, and T. Pataki: *J. Mater. Eng. Perform.*, 2014, vol. 23, pp. 2347–50.
- D.L. Beke, L. Daróczi, and T.Y. Elrasasi: Shape Memory Alloys-Processing, Characterization and Applications, InTech, London, 2013, pp. 167–96.
- D.L. Beke, L. Daróczi, L.Z. Tóth, M.K. Bolgár, N.M. Samy, and A. Hudák: Metals, 2019, vol. 9, pp. 58–81.
- V. Mertinger, M. Benke, and E. Nagy: *Mater. Today Proc.*, 2015, vol. 2, pp. S673–76.

Publisher's Note Springer Nature remains neutral with regard to jurisdictional claims in published maps and institutional affiliations.